J Incl Phenom Macrocycl Chem (2013) 76:201–211
DOI 10.1007/s10847-012-0192-y

ORIGINAL ARTICLE

Structural evidence of differential forms of nanosponges of beta-cyclodextrin and its effect on solubilization of a model drug

Shankar Swaminathan · Pradeep R. Vavia · Francesco Trotta · Roberta Cavalli · Simonetta Tumbiolo · Luca Bertinetti · Salvatore Coluccia

Received: 7 December 2011 / Accepted: 31 May 2012 / Published online: 13 June 2012

Abstract Nanosponges (NS) are a recently developed class of hyper-branched polymers, nano-structured to form three dimensional meshwork; obtained by reacting cyclodextrins with a cross linker like diphenyl carbonate. Herein, we report an anomalous behavior of NS with regards to physical and morphological characteristics and drug encapsulation behavior by minor synthetic modification. Two distinct forms viz. crystalline and para-crystalline of NS were identified and extensively characterized by use of high resolution transmission electron microscopy (HR-TEM), X-ray powder diffraction (XRPD), scanning electron microscope, atomic force microscope, optical microscope and Fourier transform infra-red attenuated total reflectance spectroscopy (FTIR-ATR). Dimension of the crystal lattice was found to be equal to 0.61 nm. Higher magnifications clearly showed a zone axis with a hexagonal symmetry as that of beta-cyclodextrin. XRPD patterns were in concurrence with the HR-TEM results. Solubility studies with a model drug dexamethasone (DEX) showed more than three folds increase in the solubility of the drug in the crystalline NS as compared to the para-crystalline ones. Percent drug association and drug loading for DEX was found to be higher in the crystalline type of NS. An In vitro drug kinetic study evidenced a faster release of DEX from the crystalline type NS. The particle sizes of the formulations were as follows: crystalline NS: 688.6 ± 38.0 nm, para-crystalline NS: 702.2 ± 21.2 nm with polydispersity indices of 0.155 and 0.132; zeta-potential of −26.55 ± 1.7 and −23.42 ± 2.1 respectively. Differential scanning calorimetry and thermogravimetric analysis revealed that both forms encapsulated the drug satisfactorily. FTIR-ATR and Raman spectroscopy showed weak interactions. Crystallinity of NS was thus found to be an important factor in solubilization, in vitro kinetics and encapsulation behavior and can be tuned to give a tailored drug release profile or formulation characteristics.

Keywords Beta cyclodextrin · Nanosponge · Inclusion complexation · Dexamethasone · Solubilization

S. Swaminathan · P. R. Vavia (✉)
Center for Novel Drug Delivery Systems, Department of Pharmaceutical Sciences and Technology, Institute of Chemical Technology, N.P. Marg, Matunga, Mumbai 400 019, India
e-mail: vaviapradeep@yahoo.com

S. Swaminathan · R. Cavalli
Dipartimento di Scienza e Technologia del Farmaco, Università degli Studi di Torino, Turin, Italy

S. Swaminathan
Hamilton Eye Institute, Department Of Ophthalmology, University of Tennessee Health Science Center, 930 Madison Avenue, Memphis, TN 38163, USA

F. Trotta
Dipartimento di Chimica IFM, Università degli Studi di Torino, Turin, Italy

S. Tumbiolo · L. Bertinetti · S. Coluccia
Department of IFM Chemistry and NIS Centre of Excellence, Università di Torino, via P. Giuria 7, 10126 Turin, Italy

Introduction

Nanosponges (NS) are a class of novel hyper-cross-linked, polymeric derivatives of beta-cyclodextrins (β-CD), which have been synthesized by crosslinking of β-CD with diphenyl carbonate (DFC) [1–5]. They have a proven spherical colloidal nature, reported to have a very high solubilization capacity for poorly soluble drugs by their inclusion and

non-inclusion behavior [6–12]. They have been found to be safe for oral and invasive routes and thus could serve as a potential carrier for drug delivery [2, 13]. The cyclodextrin to cross-linker ratio can be varied during their preparation to improve the drug loading and solubility. Minor synthetic modifications leading to a different crystalline form of a moiety is a very common technique used in synthetic chemistry for patent life extension of a molecule. Herein we report a case with NS, wherein minor synthetic modifications have led to an anomalous behavior with respect to its physical and morphological characteristics and solubilization of a model molecule, dexamethasone. We reported this phenomenon briefly in our earlier publication [8]. In this paper, we outline a detailed study on the same using a model drug molecule. Andrea Mele, Trotta and co-workers [14] have recently reported structural studies on a swellable type of NS, formed by cross-linking of cyclodextrin with pyromellitic anhydride. However, there are no reports on the crystal behavior or detailed characterization of NS formed by the use of DFC as cross-linker.

Dexamethasone (DEX) is a poorly soluble compound, which has been extensively used as an analgesic and an anti-inflammatory agent. A major objective of the paper is to highlight two distinct forms of NS namely crystalline and para-crystalline or amorphous (used interchangeably) by use of techniques like HR-TEM and XRPD. For further detailed elucidation, other auxiliary techniques were also used viz. SEM, TEM, AFM, OM and FTIR-ATR. DEX was complexed with both forms of NS separately by an incubation method followed by lyophilization to obtain NS loaded with DEX. The differential solubilization and encapsulation behavior by NS were assessed by physicochemical evaluation, solubilization studies, and in vitro release kinetic studies of NS-DEX formulations. Dexamethasone, due to its poor solubility and hydrophobic nature causes problems in its efficient clinical usage [15, 16]. For instance in the ocular applications of DEX, low residence time of formulations in the eye results in only about 5 % drug penetration and thus a need for frequent administration arises. Continuous application further leads to a plethora of problems as in glaucoma of the eye with damaged optic nerve, visual disturbances, subcapsular cataract generation and corneal thinning [17–21]. A carrier based system like NS may serve to increase the residence time of drug in the eye and also may release the drug in a controlled manner thereby also reducing the associated side effects [22, 23]. Cyclodextrins have found some applications in ophthalmology, but NS has not been utilized for this purpose yet. The work in this paper would also be used as a base paper for formulation of a NS based ocular drug delivery system of DEX.

Materials and methods

Materials

β-CD was obtained from Wacker Chemie, (Munich, Germany). DFC and DEX were purchased from Sigma Aldrich (Milan, Italy). All other chemicals and reagents were of analytical grade. Milli Q water (Millipore, USA) was used throughout the studies.

Synthesis of β-CD NS

β-CD NS were prepared using DFC as cross-linker by a previously reported method [1, 2]. Briefly, anhydrous β-CD, 1.135 g (0.001 mols) and 0.856 g (0.004 mols) of DFC were dissolved in 100 ml Dimethyl sulfoxide in a 250 ml flask. The flask was placed in an ultrasound bath filled with water and heated to 90 °C. The mixture was sonicated for 12 h. The reaction mixture was left to cool; the product obtained was broken up with spatula and was washed with water in order to remove the non-reacted cyclodextrin and then was washed in soxhlet with absolute ethanol (99.9 %v/v) to remove the phenol developed and the residual DFC. The product obtained is a fine white powder insoluble in water and common organic solvents.

The purified product was stored at 25 °C until further use. This reaction was also carried out in the absence of ultrasound.

Structural characterization of NS

Scanning electron microscopy

A Leica Stereoscan scanning electron microscope (SEM) with tungsten filament and thermionic emission, 3–30 keV acceleration tension and 50 nm of resolution was used for morphological analysis. Samples were prepared by sprinkling NS powder on a double-sided carbon adhesive tape mounted on a sample holder, and then sputtered with a thin film of gold to minimize the charging effects.

X-ray powder diffraction

To understand the differential crystallinity behavior of NS better, we carried out a detailed XRPD study using both a Huber Guinier CameraG670 (simultaneous collection of reflections between 7 and 100° at 2θ) and a Siemens D5000 diffractometer (Bragg–Brentano geometry, sequential collection between 2.5 and 60° at 2θ). For ease of understanding, the areas were divided into integrals and Full width at half maximum was used as a comparative parameter.

High resolution transmission electron microscopy (HR-TEM)

HR-TEM was performed with a JEOL JEM-3010 microscope operating at 300 kV (Cs = 0.6 mm, point resolution 1.7 Å). Images were recorded with CCD camera (Multi-Scan model 794, Gatan, 1,024 × 1,024 pixels, pixel size 24 × 24 μm^2). The powdered samples were ultrasonically dispersed in propanol and the obtained suspensions were deposited on a copper grid, coated with a porous carbon film. Both the types of NS were subjected to these studies for the crystal structural elucidation.

The results obtained were correlated with XRPD studies using the in-built software of the system.

Conventional TEM

Conventional TEM analysis was performed using a Philips CM 10 transmission electron microscope using magnification 72000×. The sample was prepared by a formvar resin grid method. Briefly, a 0.5 % w/v suspension of NS was sprayed on a formvar resin coated TEM grid and air dried for 10 min before observation. The negative films (Kodak SO163) were digitized off line using Kodak mega plus CCD camera. Contrast enhancement and particle measurement were performed using the NIH image software.

Atomic force microscopy

A further in-depth morphological analysis was performed using a DME Dualscope Rasterscope C21 Atomic Force Microscope (alternate contact mode, Mikromash Si tips, Au-backside, k = 15 N/m) with a Scanner of 50 μm with three piezo electrodes for three axes X, Y and Z in anon-contact mode. Silicon tips had an elastic constant of 40 nm equipped with Dual scope DS 95-50 camera. The data was processed using SPM software. The sample suspensions (1 %w/v) were prepared in distilled water and a drop was impregnated onto aluminum sheet (2 × 2 cm). This was allowed to dry in a HEPA filter zone and the dried region was analyzed.

Fourier transform infrared-attenuated total reflectance spectroscopy (FTIR-ATR)

FTIR-ATR was performed using a Perkin Elmer system 2000 spectrophotometer, to understand if there exists any structural difference between the two forms of NS. The spectra were obtained, using KBr pellets for sample preparation method in the region 4,000–650 cm^{-1}.

Optical microscopy

The NS suspensions (0.5 %w/v) were observed using a Leitz invert microscope, following suitable dilution with water, to evaluate the particle distribution after dispersion.

Preparation of DEX loaded NS

Loading of DEX in both types of NS was done using incubation method followed by lyophilization of the drug loaded NS. Accurately weighed quantities of NS were suspended in 20 ml of MilliQ water using a magnetic stirrer, after which calculated amount of DEX was dispersed in a ratio of 1:6 (DEX to NS by weight) and were stirred for 24 h. After 24 h, the suspensions were centrifuged at 2,000 rpm for 10 min to separate the un-dissolved drug as a residue below the colloidal supernatant. The colloidal supernatants were lyophilized at −20 °C and at an operating pressure of 13.33 mbar to obtain drug-loaded NS formulations.

Determination of DEX loading in NS

Weighed amounts of DEX loaded NS were extracted with methanol under sonication and diluted suitably with ethanol/water mixture and were analyzed by HPLC. HPLC analysis was performed employing an HPLC apparatus (Shimadzu, Tokyo, Japan) consisting of a SPD-2A UV–Vis detector, a LC-6A pump unit control, a C-R3A chromatopac integrator and a RP-C18 column (250 mm, 5 μ packing, 4.6 mm i.d.). The mobile phase for elution was acetate buffer pH 4.8 and acetonitrile (67:33). A wavelength of 246 nm was chosen for analysis. The retention time of DEX was found between 12 and 13 min. The method was validated for parameters like linearity, limit of detection, and quantitation.

We devised a formula to assess the drug association with NS by factoring in the yield of formulation batch as well. This term is referred to as "percent drug association" which was calculated using the following formula (performed in triplicate):

$$\frac{C \times M \times 100}{T \times W}$$

where C is the concentration of DEX obtained by HPLC in mg, M is the total particle mass—the yield of the formulation, T is the particle mass tested—weight of NS formulation used for quantification of DEX, W is the initial weight of the drug fed for loading—Known amount of drug used for formulation.

Solubility studies

Excess amounts of DEX were incubated with increasing amounts of each type of NS (0–0.2 %w/v) at room

temperature and were subjected to mechanical stirring for 24 h. The suspensions were then centrifuged for 10 min at 10,000 rpm to separate the free DEX and encapsulated DEX with the colloidal supernatants encapsulating the drug were then analyzed for DEX by HPLC according to the afore mentioned method.

Physico-chemical characterization of DEX-loaded NS

FTIR-ATR

FTIR-ATR was performed using a Perkin Elmer system 2000 spectrophotometer, to understand if there exists some interaction between drug and NS. The spectra were obtained, using KBr pellets, in the region from 4,000 to 650 cm^{-1}.

Raman spectroscopic (RS) analyses

RS analyses were made using Jasco (Japan) make Raman system R-3000, with a 10 cm^{-1} resolution, laser wavelength of 785 nm and a range of 200–2,400 cm^{-1}. Interaction/encapsulation would result in a diminished peak in the spectra of formulations.

Differential scanning calorimetry (DSC)

DSC was carried out by means of a DSC 2010 differential scanning calorimeter (TA instruments Inc., USA). The instrument was calibrated with indium for melting point and heat of fusion. A heating rate of 10 °C/min was employed in the 35–300 °C temperature range. Standard aluminum sample pans (Perkin-Elmer) were used; an empty pan was used as reference standard. Analyses were performed in triplicate on 5 mg samples under nitrogen purge. It was performed with a rationale to understand whether there was an inclusion of DEX into NS.

Thermogravimetric analysis (TGA)

TGA was performed using TGA 2050 thermogravimetric analyzer (TA instruments Inc., USA). The temperature range was 35–450 °C. Around 8–10 mg of sample was placed on a sample pan and subjected to the above mentioned program under a nitrogen atmosphere.

Particle size and zeta potential measurement

Particle sizes and polydispersity indices of NS based formulations were measured by dynamic light scattering using a 90 Plus particle sizer (Brookhaven Instruments Corporation, USA) equipped with MAS OPTION particle sizing software. The measurements were made at a fixed angle of 90° for all samples. The samples were suitably diluted with Milli Q water for every measurement. Zeta potential measurements were also made using an additional electrode in the same instrument. For zeta potential determination, samples of the three formulations were diluted with 0.1 mM KCl and placed in the electrophoretic cell, where an electric field of about 15 V/cm was applied. The mean hydrodynamic diameter (Dh) and polydispersity index (PI) of the particles were calculated using the cumulant analysis after averaging the three measurements.

In vitro release of DEX from NS formulations

The in vitro release was carried out using multi-compartment rotating cells with a dialysis membrane (cut off 12,000 Da). The donor phase consisted of formulations containing a fixed amount of DEX (250 μg/ml) in phosphate buffer at pH 7.4 (1 ml). The receiving phase also consisted of phosphate buffer, pH 7.4. The receiving phase was completely withdrawn and replaced with fresh medium after fixed time intervals, suitably diluted and analyzed using the HPLC method as described before.

Results and discussions

NS are hyper-crosslinked cyclodextrin polymers consisting of solid nanoparticles with colloidal sizes and nanosized cavities. These nanostructured materials can form inclusion and non-inclusion complexes with different compounds and formed a nanosuspension of rather uniform spherical shaped nanoparticles after dispersion in water under stirring. NS structural characterization [2, 24] had shown that the carbonate linkage was added to the primary hydroxyl groups of the parent β-CD unit. Thus the drug molecules could be included into the nanocavities of β-CD and, due to the crosslinking further interactions of the guest molecules with more β-CD units are probable. Moreover, the presence of the crosslinks might also form nanochannels within the NS structure of the polymer mesh. This peculiar structural organization might be responsible for the increased solubilization and protection capacities of NS in comparison with the parent cyclodextrin. In the formulation stages of complexes, we serendipitously found out that different batches of NS (synthesized with slight variations) solubilized the drugs in varying proportions. Further investigations led to the discovery of the fact that the differential solubilization properties of the NS using different synthetic techniques could be due to the differences in the crystal nature of NS.

As a matter of fact, ultrasonication-assisted synthesis led to the formation of a typical crystalline type of NS with definite crystal phases separated by a fixed distance on an

amorphous background. A preliminary characterization of the bulk NS was performed using XRD, SEM, AFM and HR-TEM.

As shown in the SEM images reported in Fig. 1a, β-CD NS present crystalline morphologies only when carried out under particular conditions, i.e. under ultrasound irradiation, as opposed to a disorganized structure obtained without ultrasound as seen in Fig. 1b. The synthesis of β-CD NS produces systems with specific ordered structures, whose X-ray diffraction patterns, marked by series of peaks on an amorphous background, show a long-range order (Fig. 2).

In Fig. 3a, poorly crystalline NS, obtained from β-CD cross-linked (1:4 β-CD/cross-linker agent ratio), are compared with that of a well crystallized NS having the same cross-linker ratio.

In Fig. 3b, c, XRPD pattern decomposition shows some broad reflections in the paracrystalline phase that appear as narrowpeaks in the crystalline sample.

Poorly crystalline NS formed using different β-CD crosslinking ratio show very similar XRPD patterns (data not shown). But the decomposition of the XRPD diagrams of these types of NS underlines the crystallinity degree of the NS with a weak long range order characterized by some broad reflections indicated in Fig. 3; the short range order being almost lost and represented only by a small peak at 34.24° (2θ). The ratio of intensity to full width at half maximum (I:FWHM) also differed considerably in both types of NS (Table 1). A detailed overlap of the XRD of crystalline and para-crystalline NS was done and, for simplification, it was divided into three integrals (Fig. 4). It was found that both the forms of NS exhibit a very similar pattern of diffractogram on a whole but it largely differed in the areas of the peaks and also the peak intensities (Table 2). NS samples are dramatically unstable under the electron beam of the microscope. However, the HR-TEM analysis has shown ordered areas of restricted dimensions (10–50 nm) on an amorphous phase (Fig. 5).

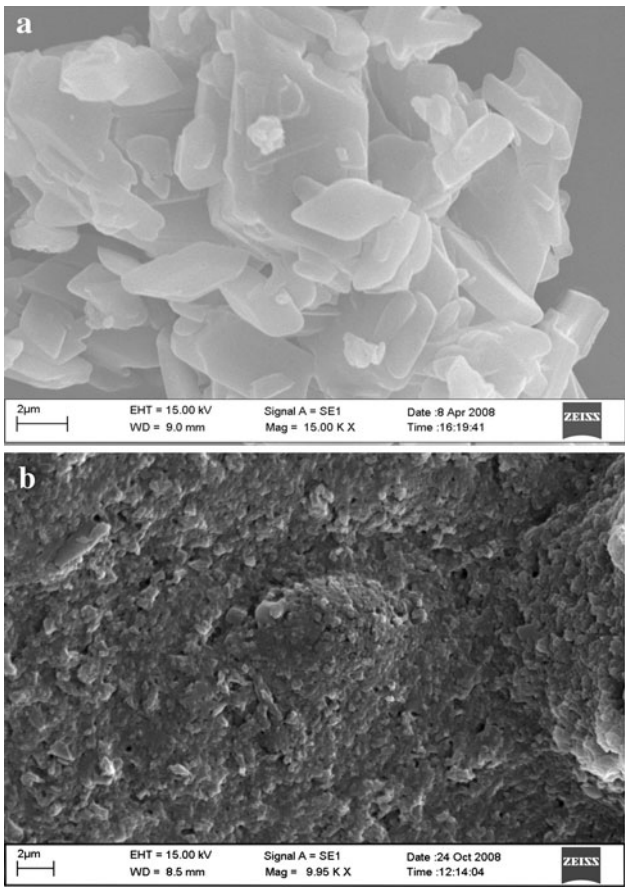

Fig. 1 SEM images of **a**. Crystalline type of NS. **b** Paracrystalline type NS

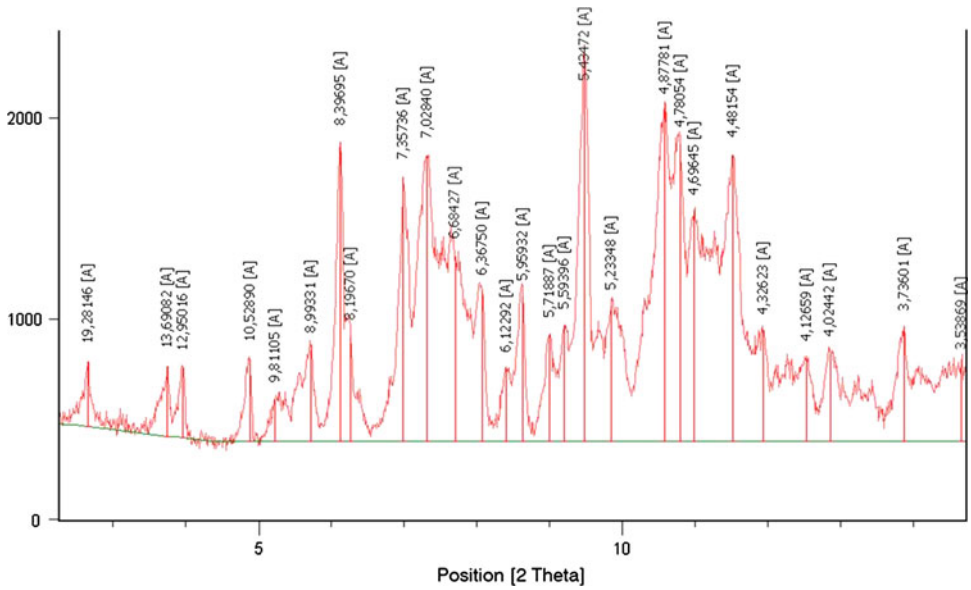

Fig. 2 XRD pattern of a β-cyclodextrin NS sample with long range order of the structure

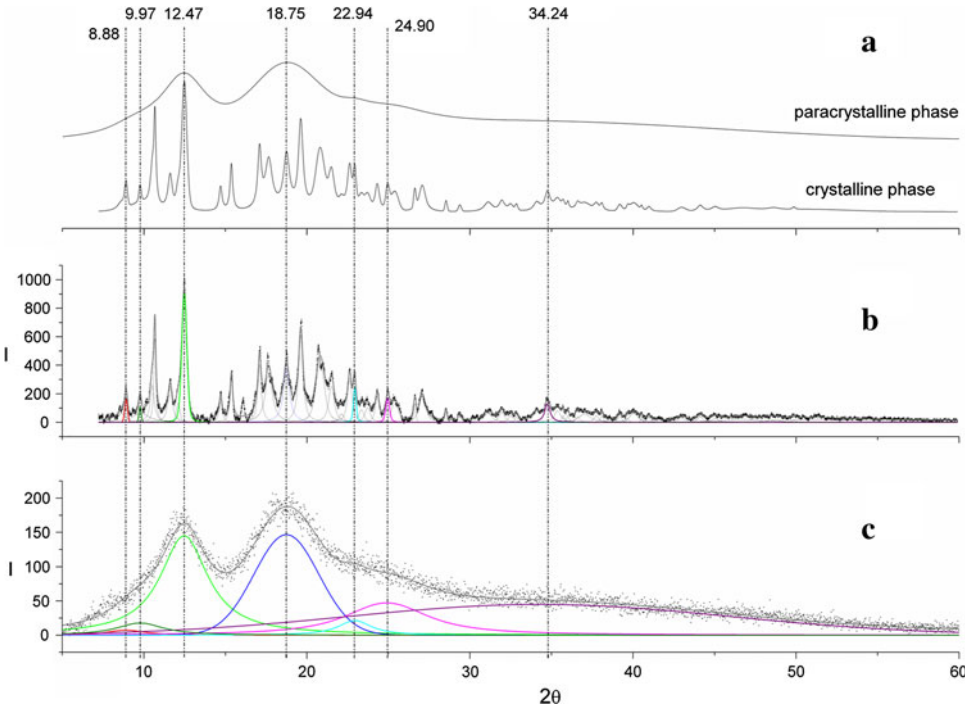

Fig. 3 **a** Poorly crystalline NSs from β-CD polymerized (1:4 β CD/crosslinker agent ratio) compared with the well crystallized ones at the same cross-linker ratio (**b**). XRPD pattern decomposition shows some broad reflections that appear as narrow peaks in the crystalline sample (**c**)

Table 1 Peak position recurrence between poorly crystalline NS sample and crystalline NS sample and intensity v/s FWHM ratios

Peak position	Para crystalline sample		Crystalline sample	
(2θ)	Area	I/FWHM	Area	I/FWHM
8.88	32.23	2.59	102.56	544.26
9.77	94.80	5.10	54.36	10189.73
12.47	807.58	40.86	436.64	2343.21
18.75	731.34	31.32	330.27	792.99
22.94	80.82	8.76	49.17	3389.02
24.90	427.23	7.78	69.71	641.95
34.24	1318.59	1.62	244.04	68.93

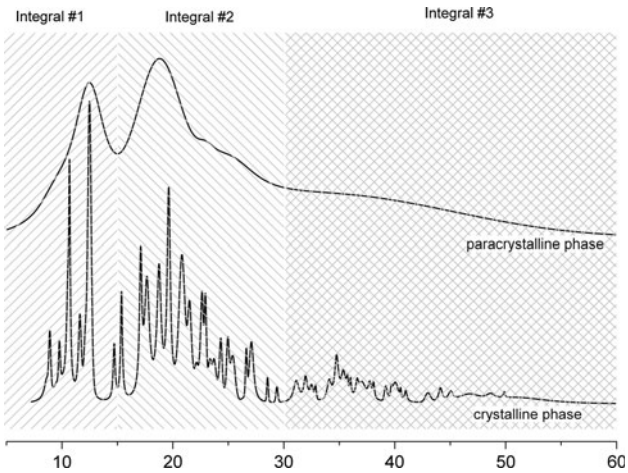

Fig. 4 Overlap of XRP diffractograms for 2θ interval for the integral evaluation

The d-spacing marked out in each HR-TEM image matches perfectly with those calculated from the XRD pattern. Figure 6 further elucidates the presence of an ordered structure characterized by a zone axis with hexagonal symmetry due to the structure of β CD. Conventional TEM studies could focus on a single crystal of NS elucidating its definite crystalline geometry, while the amorphous NS were found to have a spherical shape (Fig. 7). AFM studies showed that the crystalline NS showed presence of prominent crystal planes with an average height of around 500 nm, (Fig. 8a). Paracrystalline NS showed presence of nearly spherical colloidal particles with an average height of around 600 nm (Fig. 8b). Excluding the artifacts, the particle sizes were in the range of 400–600 nm in both forms.

FTIR-ATR showed a slight peak shift for C=O bond of the crystalline type of NS by about +40 at 1780.05 cm^{-1} (Fig. 9). Optical microscopic results were used as a preliminary tool for characterization in the developmental stages. They showed the presence of distinct crystals as opposed to roughly spherical structures of amorphous NS. These two distinct types of NS were further individually evaluated for solubilization of a model molecule DEX.

Different packing's of DEX in the crystal structure of NS complexes might affect physical and pharmaceutical properties of DEX as drug loading, drug stability and drug release.

Table 2 Areas measured over the previously indicated 2θ ranges

	2θ range (degrees)	Paracrystalline phase (P)	Crystalline phase (C)	Area ratio (C/P)
Integral#1	7.5–15	799.1	1187.6	1.49
Integral#2	15–30	1668.3	2521.8	1.51
Integral#3	30–60	980.6	1488.7	1.52

The multiplication factor (1.5) is closely related to the instrumental enhancement

The observed differences may be related to the presence of channels or cavities running through the NS crystal structure and working as sites for DEX molecules in addition to cyclodextrin cavities. When the crystal structure of the NS collapses, as **is** the case of the paracrystalline NS, the beehive-like structure of the complex fails and the DEX molecules lose their preferential crystallographic sites. This outcome is confirmed by the observation that DEX loading is higher in the crystalline NS than in paracrystalline NS.

For the estimation of drug association with NS, we assessed the drug loading, i.e. the amount of drug encapsulated into NS, calculated by analyzing a fixed amount of formulation by HPLC as per the method given in Sect. 2.5, percent drug association which is calculated by a formula given in Sect. 2.5, and effect of NS on the solubility characteristics of DEX as mentioned in Sect. 2.6.

Percent drug loading with crystalline NS was found to be $\sim$25 % w/w [%cumulative variance (CV) = 0.6] and that with paracrystalline NS was found to be $\sim$20 % w/w (%CV = 0.7). The percent drug association in crystalline type NS was found to be around 10 % (%CV = 0.3) as compared to around 6 % (%CV = 0.5) in the paracrystalline type suggesting that probably the crystal structure of NS plays a very important role in DEX complexation. The importance of the crystalline structure on NS complexation ability is under investigation showing its marked influence also with other types of active molecules. Solubility studies confirm the hypothesis as more than 2 mg/ml of DEX was

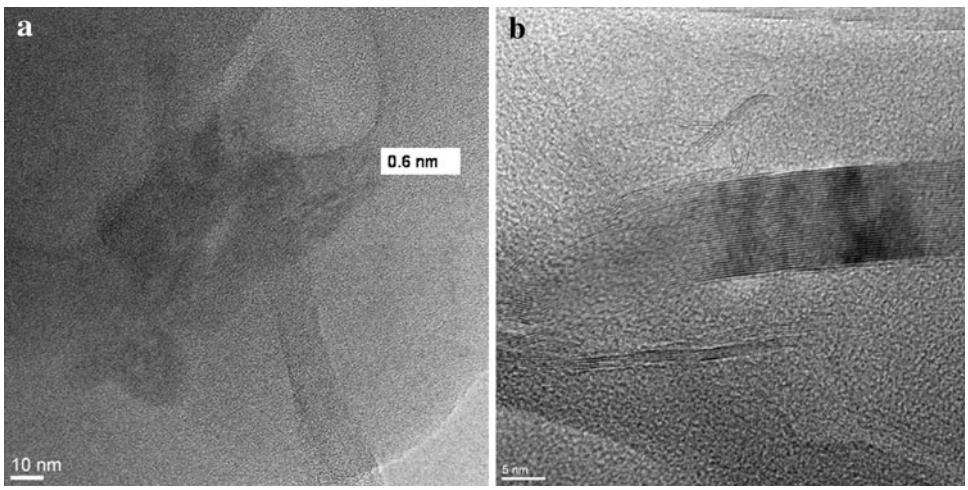

Fig. 5 HR-TEM images of β-cyclodextrin NS samples showing ordered areas of restricted dimensions (10–50 nm) on an amorphous phase in lower magnification (**a**) and higher magnification (**b**)

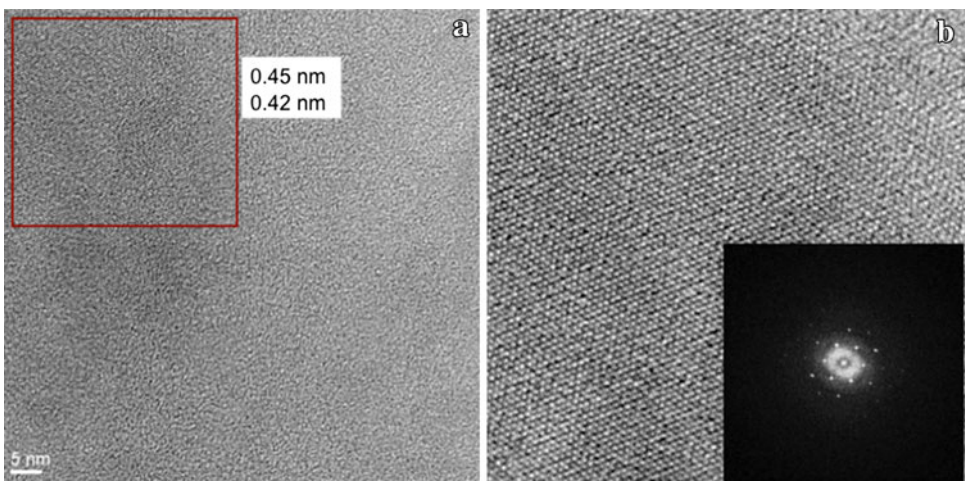

Fig. 6 HR-TEM micrographies of the structure of a β-cyclodextrin sample in a lower magnification (**a**) and high magnification (**b**). The diffraction pattern in the inset shows the ordered sample structure characterized by a zone axis with hexagonal symmetry probably due to the structure of the β-cyclodextrins

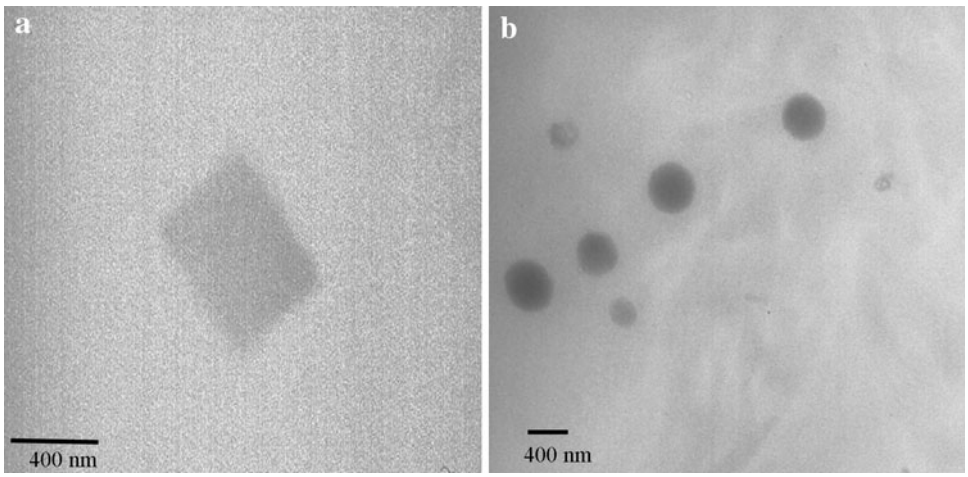

Fig. 7 Conventional TEM images of NS (×72,000). **a** Crystalline type, **b** paracrystalline type

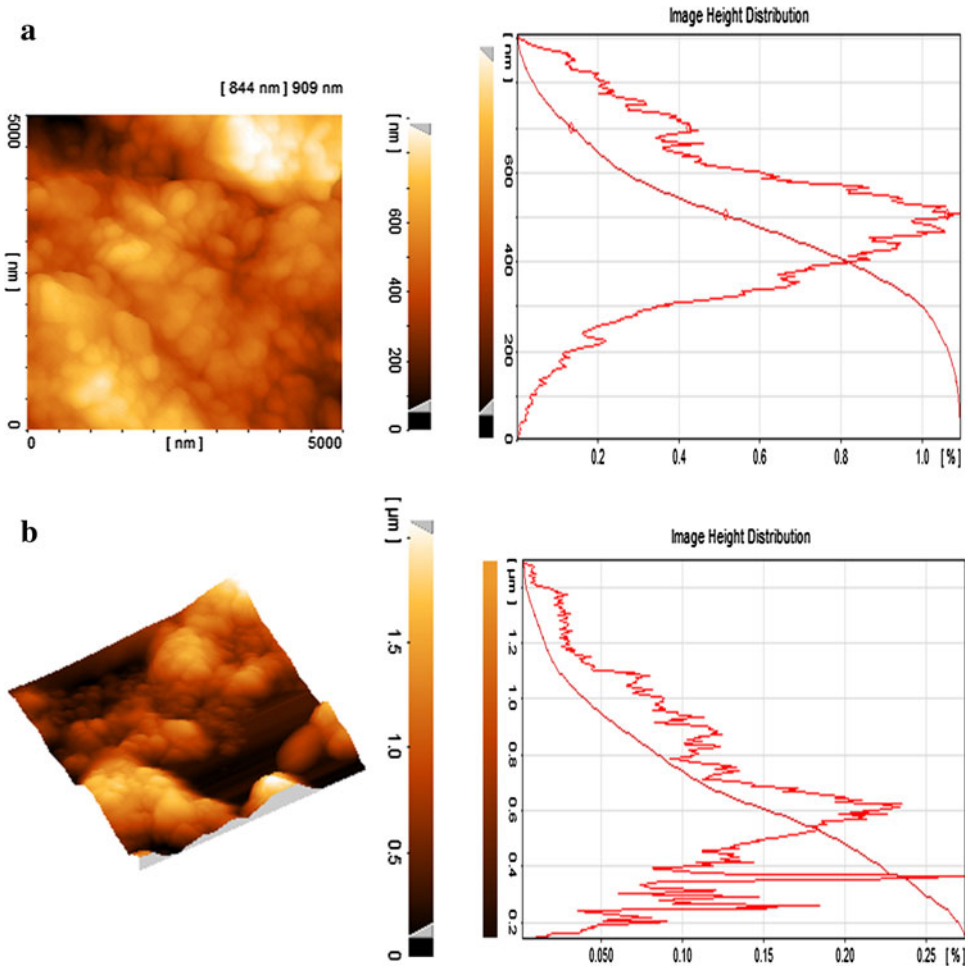

Fig. 8 AFM images of **a**. Crystalline NS and **b**. Paracrystalline NS

encapsulated by NS crystalline as compared to around 0.6 mg/ml by NS paracrystalline as measured by HPLC.

FTIR-ATR studies of the complexes clearly showed significant interactions of DEX with NS crystalline as well as NS paracrystalline type (Fig. 10). The major peaks of DEX were seen at 900, 1050, 1600, 1700 and 1720 cm^{-1} which were masked/broadened on complexation. The sensitivity of the technique was not sufficient enough to differentiate interactions between the two types of NS.

Raman Spectroscopy has proved to be a very important tool in the recent years has for studying interactions of drug and polymers. There are not many reports of the same

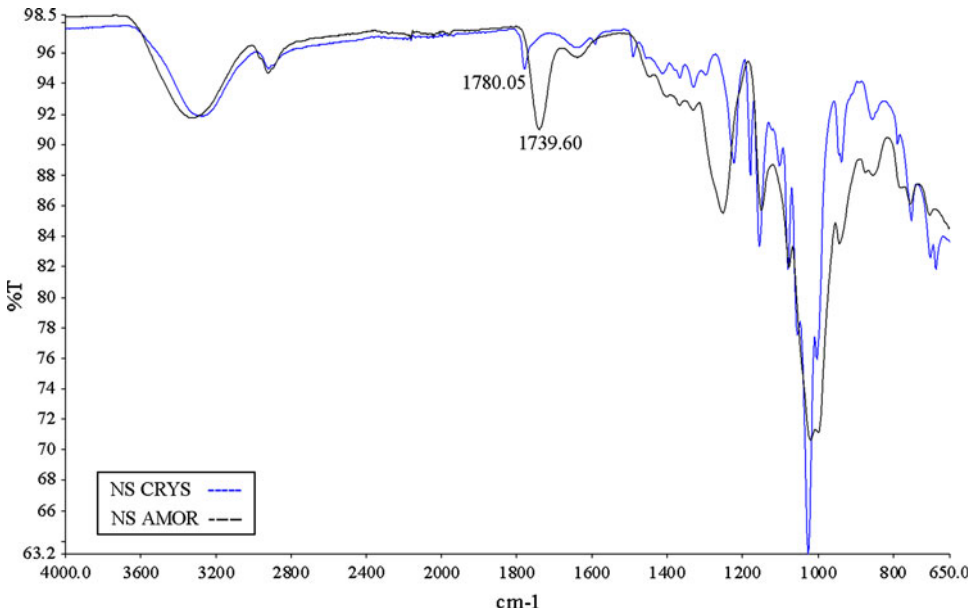

Fig. 9 FTIR-ATR of crystalline NS and paracrystalline NS

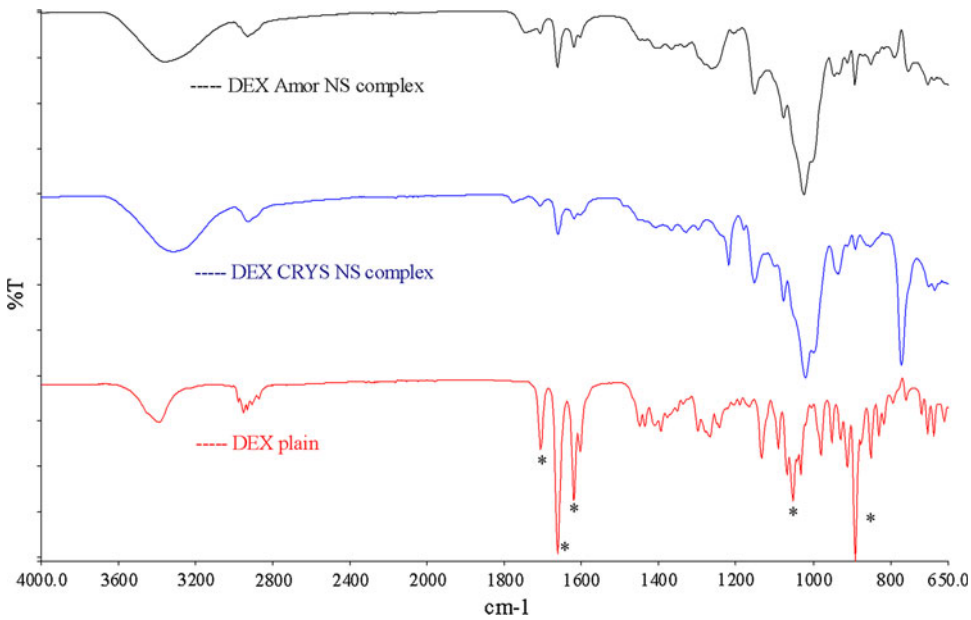

Fig. 10 FTIR-ATR of DEX complexes

using β-CD and drugs and this is the first time that we are attempting to study interactions of NS and a drug using Raman Spectroscopy. It was observed that important Raman markers of DEX such as peaks at 1620, 1480, 1440, 950 and 680 cm^{-1} were substantially masked or displaced on complexation with NS (Fig. 11). Both the spectroscopic techniques used in conjunction provided a better picture to understand the interactions of DEX and NS.

Thermal methods viz. DSC and TGA were used to understand the holistic picture of true encapsulation. In some of our previous studies we found that there was a possibility of formation of non-inclusion complexes of drug molecules with NS [2, 8]. It was also proposed that there may exist peripheral interactions which are responsible for the same. Herein as we see in Figs. 12 and 13, the DSC and TGA curves of the formulations of DEX show that the endotherms for the DEX were masked completely in case of drug NS formulation supporting the fact that there is a true encapsulation seen in case of DEX and NS. DSC gives a measure of the change in enthalpy and TGA gives a measure of change in weight of the sample on heating. Both these studies used in conjunction enabled us to conclude that there is an internalization of DEX within the NS matrix. It may thus seem from FTIR-ATR, Raman studies, DSC and TGA that DEX associates more or less in a similar way with both forms of NS but the orientation

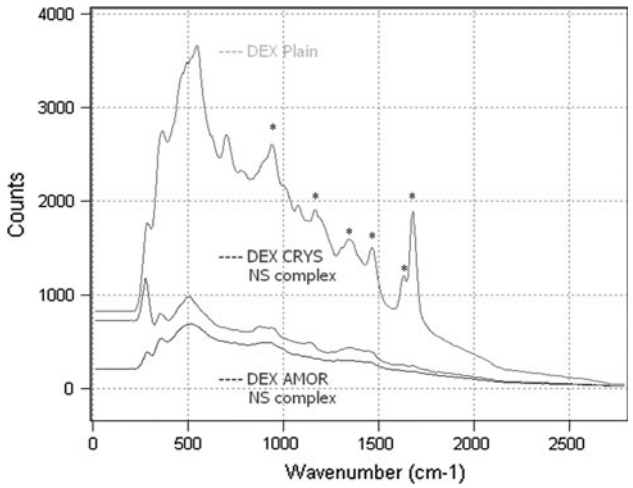

Fig. 11 Raman spectroscopic studies of DEX complexes

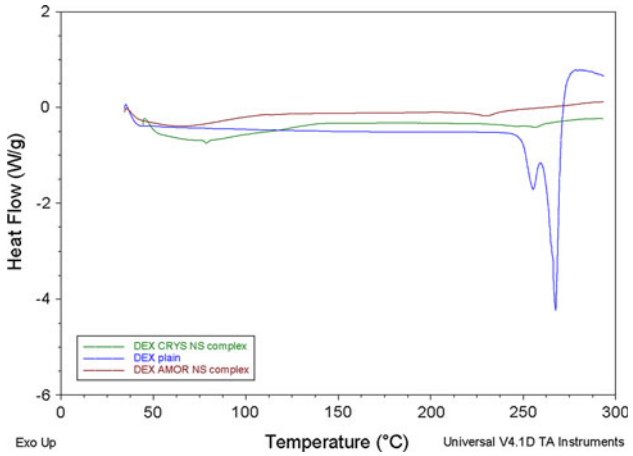

Fig. 12 DSC theremogram of complexes of DEX

inside the crystal matrix is of paramount importance for effective solubilization. In absence of the effective crystal phases, DEX orients perhaps in a random manner thus

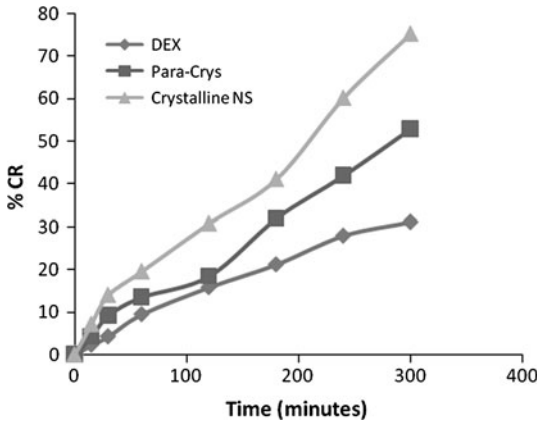

Fig. 14 In vitro release studies of DEX complexes

leading to less effective solubilization. The crystal structure of NS thus plays an important part in solubilization of this particular molecule.

The size ranges for both the complexes were between 400 and 500 nm. These studies were in agreement with the laser light scattering technique. The particle sizes and zeta-potential of NS-CRYS complex was found to be 688.6 ± 38 nm (PI = 0.155, Z.P. = −26.55 ± 1.7 mV) and that of NS-PARA complex was found to be 702.2 ± 21.2 nm (PI = 0.132, Z.P. = −23.42 ± 2.1 mV). A sufficiently high ZP indicates that the complexes would be stable and the tendency to agglomerate would be miniscule. A narrow PI means that the colloidal suspensions are homogenous in nature.

In vitro dissolution studies supported the previous hypothesis of association of DEX in NS (Fig. 14). It was seen that DEX was released faster from the crystalline complex as compared to the paracrystalline NS system. The overall in vitro drug release enhancement from the DEX-Crystalline NS system was around three to four folds as compared to plain DEX. Enhanced solubilization and subsequent release of DEX from the NS is mainly due to

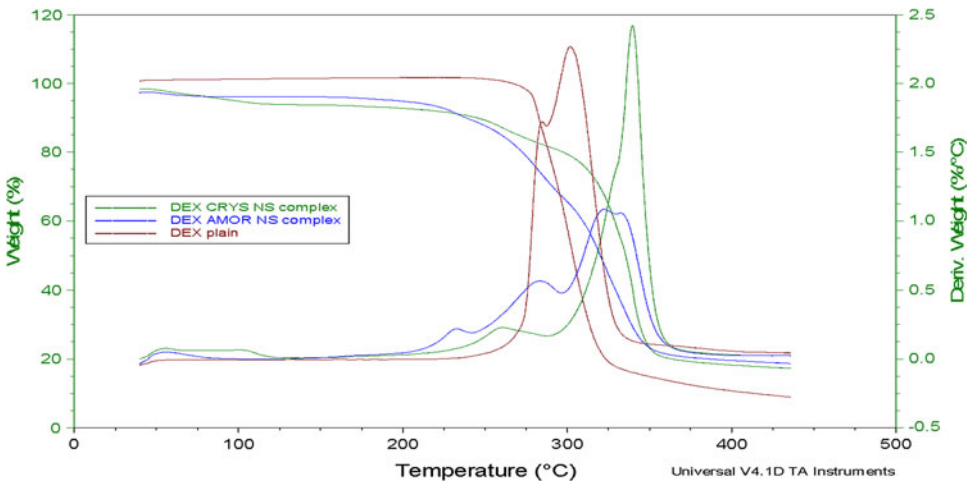

Fig. 13 TGA theremogram of complexes of DEX

the inclusion of DEX into the cavities of β-CD present in NS as well as the nano-channels within the colloidal matrix of NS. This, along with a subsequent reduction of particle size to a nanometric range culminated in solublization of DEX.

Conclusions

NS were obtained in two different crystalline forms viz. crystalline and paracrystalline/amorphous form. In-depth characterization studies confirmed the existence of both the forms. The anomalous solubilization behavior of the two forms was also studied in detail using a model molecule DEX. It can be postulated that DEX was internalized within the colloidal matrix of NS, in addition to the β-CD cavities, which helps in additional DEX solubilization and loading. Enhanced solubilization by crystalline NS may be attributed to the better orientation of DEX in a well defined crystal matrix of NS and also inside the nano-channels of NS, thus providing an increased effective surface area. Additionally the particle size of the crystalline formulation was also lesser than the para-crystalline ones. Solubilization of poorly soluble molecules by use of NS could serve as a platform technology which may also offer patentability options for the formulators.

Acknowledgments The authors would like to acknowledge Prof. Aquilano and Dr. Linda Pastero for their help in X-ray studies. The authors are thankful to M/s Sea Marconi Inc. Colegno, Italy, All India Council of Technical Education and National Facilities in Engineering and Technology with Industrial Collaboration for the funding and facilities respectively.

References

1. Trotta, F., and Tumiatti, W.: WO 03/085002 (2003)
2. Swaminathan, S.: Studies on novel dosage forms. Masters of pharmaceutical Sciences Dissertation submitted to the University of Mumbai (2006)
3. Trotta, F., Cavalli, R.: Characterization and applications of new hyper-cross-linked cyclodextrins. Compos. Interfaces **16**, 39–48 (2009)
4. Swaminathan, S.: Design and characterization of novel polymeric drug delivery system. Ph.D. (Tech.) Dissertation submitted to the University of Mumbai (2010c)
5. Cavalli, R., Trotta, F., Tumiatti, W.: Cyclodextrin-based nanosponges for drug delivery. J. Inclusion Phenom. Macrocycl. Chem. **56**, 209–213 (2006)
6. Swaminathan, S., Vavia, P.R., Trotta, F., Torne, S.J.: Formulation of betacyclodextrin based nanosponges of itraconazole. J. Inclusion Phenom. Macrocycl. Chem. **57**, 89–94 (2007)
7. Swaminathan, S., et al.: Novel functionalized beta cyclodextrin nanosponge based stable formulation of camptothecin and in vitro cytotoxicity evaluation. A poster presented at the Fifth Asian cyclodextrin conference in Busan, Korea (2009)
8. Swaminathan, S., et al.: Cyclodextrin-based nanosponges encapsulating camptothecin: physicochemical characterization, stability and cytotoxicity. Eur. J. Pharm. Biopharm. **74**, 193–201 (2010)
9. Swaminathan, S., et al.: In vitro release modulation and conformational stabilization of a model protein using swellable polyamidoamine nanosponges of β-cylcodextrin. J. Inclusion Phenom. Macrocycl. Chem. **68**(1–2), 183–191 (2010)
10. Vavia, P.R., et al.: Enhanced oral paclitaxel bioavailability after administration of paclitaxel-loaded nanosponges. Drug Deliv. **17**(6), 419–425 (2010)
11. Vavia, P.R., et al.: Paclitaxel loaded nanosponges: in vitro characterization and cytotoxicity study on MCF-7 cell line culture. Curr. Drug Deliv. **8**(2), 194–202 (2011)
12. Ansari, K.A., Vavia, P.R., Trotta, F., Cavalli, R.: Cyclodextrin-based nanosponges for delivery of resveratrol: in vitro characterization, stability, cytotoxicity and permeation study. AAPS Pharmsci. Tech. **12**(1), 279–286 (2010)
13. Vavia, P.R., Swaminathan, S., Trotta, F., and Cavalli, R.: Applications of nanosponges in drug delivery, XIII international cyclodextrin symposium, Turin (2006)
14. Andrea, M., et al.: HR MAS NMR, powder XRD and Raman spectroscopy study of inclusion phenomenon in β CD nanosponges. J. Inclusion Phenom. Macrocycl. Chem. **69**(3–4), 403–409 (2010)
15. Kim, J., Chauhan, A.: Dexamethasone transport and ocular delivery from poly(hydroxyethyl methacrylate) gels. Int. J. Pharm. **353**, 205–222 (2008)
16. Clark, A.F., Yorio, T.: Ophthalmic drug discovery. Nat. Rev. Drug Discov. **2**, 448–459 (2003)
17. Melby, J.C.: Drug spotlight program: systemic corticosteroid therapy: pharmacology and endocrinologic considerations. Ann. Intern. Med. **81**, 505–512 (1974)
18. Schwartz, B.: The response of ocular pressure to corticosteroids. Int. Ophthalmol. Clin. **6**, 929–989 (1966)
19. Urban, R.C., Cotlier, E.: Corticosteroid-induced cataracts. Surv. Ophthalmol. **31**, 102–110 (1986)
20. Li, C.C., Chauhan, A.: Modeling ophthalmic drug delivery by soaked contact lenses. Ind. Eng. Chem. Res. **45**, 3718–3734 (2006)
21. Ferrante, P., Ramsey, A., Bunce, C., Lightman, S.: Clinical trial to compare efficacy and side-effects of injection of posterior sub-Tenon triamcinolone versus orbital floor methylprednisolone in the management of posterior uveitis. Clin. Exp. Ophthalmol. **32**, 563–568 (2004)
22. Young, S., Larkin, G., Branley, M., Lightman, S.: Safety and efficacy of intravitreal triamcinolone for cystoid macular oedema in uveitis. Clin. Exp. Ophthalmol. **29**, 2–6 (2001)
23. Kwak, H.W., D'Amico, D.J.: Evaluation of the retinal toxicity and pharmacokinetics of dexamethasone after intravitreal injection. Arch. Ophthalmol. **110**, 259–266 (1992)
24. Torne, S.J.: Studies on novel dosage form. Ph.D. (Tech.) Dissertation submitted to the University of Mumbai, India (2007)